Macromolecules **1984**, *17*, 2288–2295

Crystalline and Liquid Crystal Transitions of Mesogenic Polymer Mixtures and Random Copolymers

Junji Watanabe

Department of Polymer Chemistry, Tokyo Institute of Technology, Tokyo 152, Japan

William R. Krigbaum*

Department of Chemistry, Duke University, Durham, North Carolina 27706.

Received February 24, 1984

ABSTRACT: Phase diagrams were determined by DSC and a polarizing microscope for mesogenic binary homopolymer mixtures and random copolymers based on the 4,4′-dihydroxybiphenyl rigid unit. The crystalline phases and mesophases were examined by X-ray diffraction. Previous work had shown that the type of mesophase exhibited by these homopolymers depends upon the number of methylene units in the flexible dibasic acid segment. Even homologues show a smectic S_H phase, while the odd members give a smectic phase of lower order and a nematic mesophase. Hence, the number of methylene units and the even–odd character of the flexible segment were adopted as variables in this study. We find that cocrystallization of the different units is fairly frequent for mesogenic copolymers. However, copolymerization disrupts the structural regularity of the crystal, decreases the degree of crystallinity, and broadens the crystal melting transition. These effects become more prominent with increasing differences between the two repeating units, either in the length or even–odd character of the flexible segment. By contrast, the nematic or smectic mesophase can accommodate different repeating units with minimal structural disruption. The even–even copolymer having the largest difference in number of methylene units (6 and 12) displayed a monotropic nematic phase not found in either homopolymer, providing an unexpected example of polymesomorphism.

In 1975 de Gennes[1] suggested that incorporation of both a rigid and flexible segment in the repeating unit should afford polymers which exhibit thermotropic mesomorphism with controllable transition temperatures. In the same year, Roviello and Sirigu[2] investigated the properties of polyesters based on *p,p′*-dimethylbenzalazine, perhaps the first example of this type of polymer. Since that time a number of laboratories have reported the synthesis and characterization of various examples of this type of semiflexible polymer. We initially supposed that the rigid segment would determine the type of mesophase, and variation of the length of the flexible segment would only alter the transition temperature. However, subsequent experience has shown that the flexible segment can also affect the average chain conformation and hence the type of mesophase.[3-5] For example, the polyester based on 4,4′-dihydroxybiphenyl exhibits a highly ordered smectic S_H phase when the number of methylene units in the dibasic acid is even. When the number is odd, both a smectic phase of lower order and a nematic phase are found.

In view of the frequent occurrence of polymesomorphism among small molecule mesogens, it is surprising that most of the polymeric mesogens examined to date have shown only one type of mesophase. Apart from the example just cited, only the polyesters described by Bosio and coworkers,[6] and those of Galli et al.,[7] have exhibited a second mesophase. In the latter two cases the rigid segment is relatively long, which may explain the stability of more than one type of mesophase in those polymers. Perhaps future studies will lead to a better appreciation of the relationship between the chemical structure of the repeating unit and the type of mesomorphism exhibited by the polymer.

The study of binary mixtures of low molecular weight mesogens has attracted considerable attention since the earliest days of liquid crystal research. For example, over a period of years Sackmann, Arnold, and Demus[8-10] developed an identification procedure based upon mutual miscibility of binary mixtures (the contact method) which has been used to identify the 11 currently known smectic polymorphs. Mixtures have also played an important role in the technology of liquid crystal display devices by extending the range of the nematic phase to room temperature. Moreover, extrapolation of the transition temperatures of binary mixtures involving a non-mesogen sometimes provides an estimate of the virtual transition temperature of the latter component. This is a quantity of theoretical interest and one which obviously cannot be determined experimentally from study of the non-mesogen as a single component.

Polymeric systems containing two different mesogenic repeating units can be prepared in various ways. A mechanical mixture of two mesogenic homopolymers is the direct analogue of the mixtures of small molecule mesogens alluded to above. However, the two types of repeating unit can be mixed more intimately within a single chain by random copolymerization, and still other possibilities are block and graft copolymers. Copolymerization would certainly be expected to affect the transition temperatures and perhaps even the type of mesophase exhibited. The effect of different units on the structures of the crystalline and liquid crystal phases is more difficult to predict.

We have undertaken an investigation of mesomorphic properties of binary systems formed by polymer mixtures and random copolymers in the hope that these may provide additional insight into the nature of polymeric mesophases at the molecular level. We selected for this study the 4,4′-dihydroxybiphenyl rigid unit with pairs of dibasic acids having different numbers of methylene units. This choice has the advantage that the mesophase behavior of the homopolymers has been extensively studied and is well characterized, a prerequisite for the study of mesomorphism in the more complicated copolymer systems. For example, in the even-membered series the two outer X-ray reflections at 4.5 and 5.0 Å are common to all homologues, while the innermost reflection (corresponding to the smectic layer spacing) increases from 14.3 to 20.7 Å as the number of methylene units in the dibasic acid is increased from 6 to 12. Such a consistent behavior of the X-ray patterns indicates that the smectic polymorph is the same for all these homologues. This was confirmed by mutual miscibility over the entire composition range of binary mixtures of the polyesters having 10 and 12 methylene units in the dibasic acid. A further advantage of this system is that the different mesogenic behavior of the polyesters containing even and odd numbers of methylene

0024-9297/84/2217-2288$01.50/0

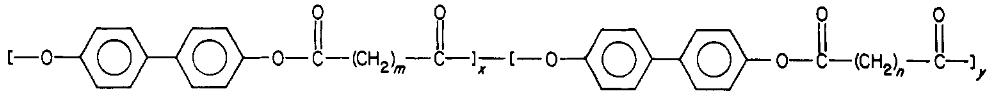

1

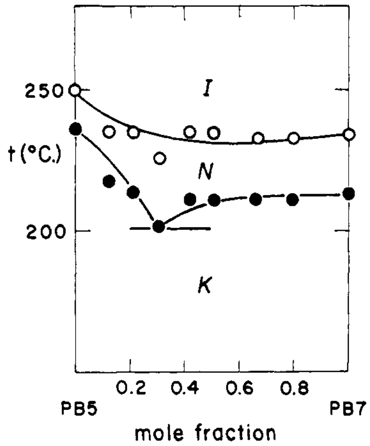

Figure 1. Simplified phase diagram for mixtures of PB5 and PB7 as determined from the DSC cooling curves.

units may provide differences among the even–even, odd–odd, and even–odd pairings in copolymers.

Experimental Section

The copolymers were prepared by melt transesterification using equimolar amounts of 4,4′-diacetoxybiphenyl and diacid. The copolymers may be represented schematically by formula 1. For brevity, this copolymer is symbolized PB-*m*,*n* where *m* and *n* are the numbers of methylene units in the two diacids. The corresponding homopolymers are designated as PB*m* and PB*n*.

Inherent viscosities were determined at 25 °C using 0.5 g/dL solutions in a 60/40 mixture by weight of phenol and tetrachloroethane. These ranged from 0.5 to 0.8 dL/g. The phase diagrams were constructed from data obtained using the DSC and a polarizing microscope equipped with a hot stage. Flat-plate X-ray pictures were recorded for the semicrystalline polymers at room temperature and for the mesophases at elevated temperatures. Details of the experimental techniques and apparatus used can be found in previous papers from this laboratory.[4,5,11-15]

Results

A. Binary Mixtures. 1. PB5 and PB7. The DSC heating curves for these mixtures show three transitions, while only two are found in the cooling curves. A similar behavior was found for the PB5 and PB7 homopolyesters, which was attributed to the existence of a monotropic smectic phase of lower order. Due to the additional transition, it proved difficult to construct the phase diagram from the heating data, so Figure 1 illustrates the simpler phase diagram for binary mixtures of these odd–odd polyesters determined from the peak temperatures of exotherms in the DSC cooling curves. This phase diagram fully conforms to expectation. In the mixtures, the crystal melting temperatures of both components are depressed (although by a relatively modest amount), leading to a eutectic composition at 0.30 mol fraction of PB7. Hence, each component crystallizes separately. Both types of crystal melt to form a nematic phase, as confirmed by the observation of schlieren textures in the polarizing microscope. The existence of a common nematic phase is in conformity with the observation for small-molecule nematic phases that all fall in a single miscibility class. One feature which might not have been anticipated is the absence of a depression of the N–I transition temperature of PB7 upon the addition of the other polymeric component. This indicates that molecules of a second polymeric nematogen can be accommodated in the nematic phase with minimal disruption of its structure.

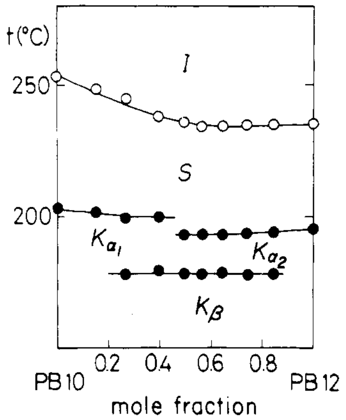

Figure 2. Phase diagram for mixtures of PB10 and PB12 from the DSC heating curves.

2. PB10 and PB12. The phase diagram of this binary mixture of even–even polymers had a similar appearance, whether determined from the DSC heating or cooling curves. We conclude that no monotropic mesophases exist. The diagram obtained using the heating data is shown in Figure 2. The smooth variation of the smectic–isotropic transition temperature indicates that both polymeric repeating units enter the smectic structure without significant disruption, and the common smectic phase extending over the entire composition range indicates (as mentioned previously) that both polymers exhibit the same smectic polymorph. This is further proven by the observation of reflections at 4.5 and 5.0 Å from the smectic phases of mixtures of all compositions. In contrast to the previous mixture, this binary system displays some unexpected features. For example, the crystal melting temperatures of PB10 and PB12 are only slightly depressed upon addition of the second component, and the two curves have a discontinuity in the center of the composition range. Moreover, an additional peak appears in the heating and cooling curves for mixtures having mole fractions of PB12 in the range 0.27–0.86. This suggests that the predominant component in the mixture crystallizes in nearly pure form, while the remainder of that component and the second component then cocrystallize in a different crystal form. However, in view of the miscibility of the two components in the smectic phase, no explanation is apparent for the very slight depression of the melting temperatures of the two single-component crystal modifications.

Figure 3 illustrates the Bragg spacings determined from the innermost reflection of the crystalline solid at room temperature and the smectic spacings measured at 215 °C. The crystal *c*-axis dimension is only slightly larger than that of PB10 over much of the composition range, leading to a curve which falls below the dashed line representing the arithmetic average. The layer spacing of the smectic phase, on the contrary, is near the larger dimension of PB12 over much of the composition range, so the curve for the mixtures lies above the dashed line representing an arithmetic average. The latter deviation might be rationalized by the fact that the smectic layer must accommodate the longer component. However, since this smectic phase is tilted, the deviation could equally well be ascribed

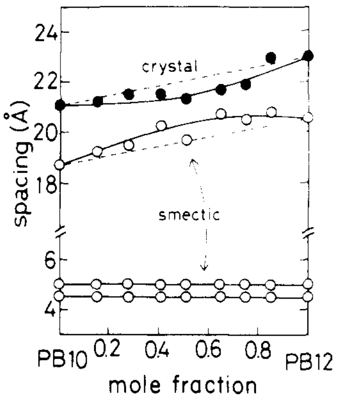

Figure 3. Bragg spacings measured for the crystalline (filled circles) phase of PB10 and PB12 mixtures at room temperature and for the smectic layer spacing (open circles) measured at 215 °C. Dashed lines represent arithmetic averages.

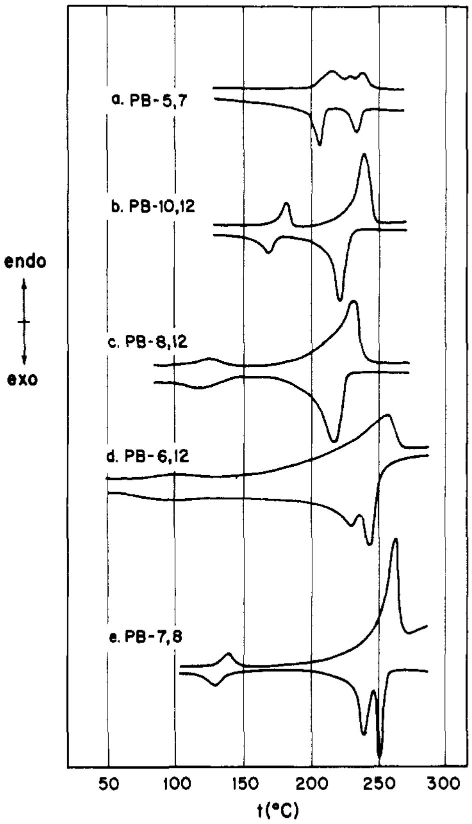

Figure 4. Typical DSC heating and cooling curves taken at 10°/min. for five copolymers have mole fractions of the first component 0.38, 0.50, 0.30, 0.50, and 0.50 (top to bottom).

to a decrease in the tilt angle (as measured from the perpendicular to the layers) for mixtures of intermediate composition. It should be noted that the smectic phases of mixtures of every composition gave quite clear diffraction patterns, indicating that the smectic structure was not seriously perturbed by the presence of two repeating units of different length. This observation supports the conclusion drawn from the smooth variation of the smectic–isotropic transition temperatures in Figure 2.

B. Copolymers. 1. Copolymer PB-5,7. A typical thermogram for this type of odd–odd copolymer is illustrated in Figure 4a for the composition having 38 mol % PB5. The DSC heating curves show three transitions, while only two are found in the cooling curves. As was the case for mixtures of PB5 and PB7 homopolymers, it proved difficult to construct the phase diagram from the heating data, so Figure 5 illustrates the simpler phase diagram based upon the DSC cooling curves. The polarizing microscopic revealed that the region between the two curves is occupied by a nematic phase which exists (on cooling) without interruption over the entire composition range. The crystal melting temperature varies smoothly with composition, indicating that the two components cocrystallize to form a solid solution. The diffraction patterns of the corresponding homopolymers (and of semiflexible chain nematogenic polymers in general) show relatively few reflections, which suggests good lateral order but poor regularity along the chain axis. This type of structure may facilitate cocrystallization of the two different repeating units. The nematic–isotropic transition temperatures also vary smoothly with composition. There may be a hint of a slight maximum in both the K–N and N–I transition temperatures for compositions low in pimelic acid.

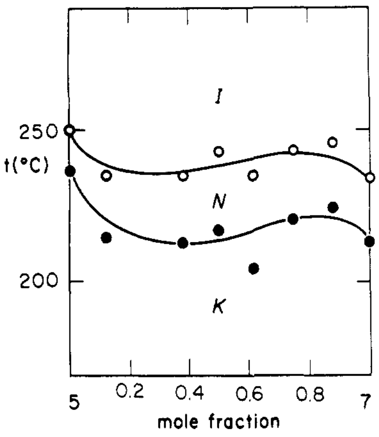

Figure 5. Simplified phase diagram based on the DSC cooling curves for PB-5,7 copolymers having different compositions.

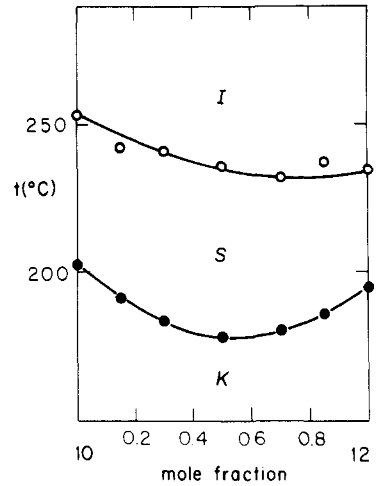

Figure 6. Phase diagram for PB-10,12 copolymers as constructed from DSC heating curves.

2. Copolymer PB-10,12. Typical DSC heating and cooling curves are illustrated for the even–even copolymer having equimolar composition in Figure 4b. Two peaks are found in both curves for all copolymer compositions and for the two homopolymers. As indicated by the phase diagram shown in Figure 6, the phases encountered with increasing temperature are crystal, smectic, and isotropic. As was the case for the mixtures of the homopolymers PB10 and PB12, an uninterrupted smectic phase exists over the entire composition range for this type of copolymer. There is only a slight depression of the melting temperature when the second component is added and no indication of eutectic behavior. This again suggests some type of cocrystallization of the two repeating units.

Table I
X-ray Data for Crystalline and Smectic Phases of 50:50 Copolymers[a]

A. Crystalline Phase (25 °C)

PB-10,12	PB-8,12	PB-6,12	PB-7,8
21.4 s	19.5 s	20 vvw (broad)	16.9 s
			14.0 w
	7.21 vvw		7.26 vvw
4.71 m	4.73 m	4.73 vw	4.79 w
4.40 m			
	4.26 s	4.28 s	4.30 s
4.20 vs			
3.90 w			
3.71 vw			3.74 w
3.47 w			3.43 vw
3.22 w			
2.96 w			

B. Smectic Phase

PB-10,12 (205 °C)	PB-8,12 (182 °C)	PB-6,12 (191 °C)	PB-7,8 (232 °C)
20.3 s	18.8 w		16.2 s
5.00 m	4.95 w	4.97 vw	5.04 m
4.51 vs	4.48 s	4.50 s	4.54 vs

[a] Values are given in Å.

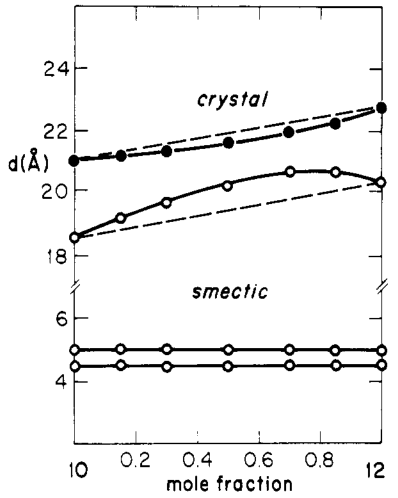

Figure 7. Bragg spacings of PB-10,12 copolymers measured for the crystalline phase at room temperature (filled circles) and for the smectic phase at 215 °C (open circles).

Table II
Enthalpies and Entropies of Transition of Copolymers Involving Tetradecanedioic Acid[a]

polymer	T_{K-S}	T_{S-I}	ΔH_{K-S}	ΔH_{S-I}	ΔS_{K-S}	ΔS_{S-I}
A. PB10, PB12, and PB-10,12 Copolymers						
PB10	203	253	2.5	4.8	5.2	9.1
85:15	191	242	1.5	4.8	3.2	9.3
70:30	189	241	1.2	4.5	2.6	8.8
50:50	178	235	1.2	4.3	2.7	8.5
30:70	180	232	1.1	4.9	2.4	9.7
15:85	186	237	2.8	5.1	6.1	10.0
PB12	194	237	3.5	5.0	7.5	9.8
B. PB8, PB12, and PB-8,12 Copolymers						
PB8	227	290	3.3	4.5	6.6	8.0
70:30	121	251	0.34	4.1	0.9	7.9
50:50	101	238	0.52	4.3	1.4	8.5
30:70	127	229	0.54	4.6	1.35	9.1
PB12	194	237	3.5	5.0	7.5	9.8
C. PB6, PB12, and PB-6,12 Copolymers						
PB6	240	336		5.0		8.1
70:30	190	276		3.0		5.4
50:50	~100	254		3.8		7.2
30:70	~170	223		3.1		6.2
PB12	194	237		5.0		9.8

[a] T values are in °C. ΔH values are in kcal/mol. ΔS values are in cal mol^{-1} K^{-1}.

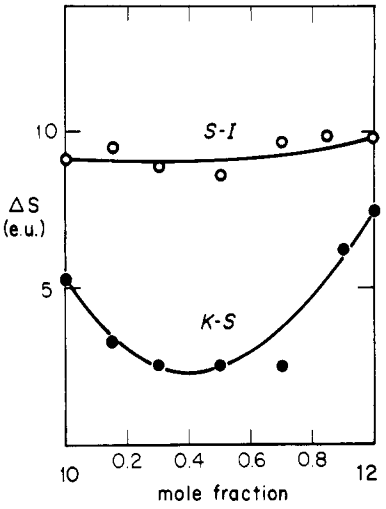

Figure 8. Entropy changes for the crystal–smectic (filled circles) and smectic–isotropic (open circles) transitions of PB-10,12 copolymers.

The Bragg spacings measured for four semicrystalline, equimolar copolymers at room temperature, and for their smectic phases at elevated temperatures, are listed in Table I. The diffraction pattern of the crystalline phase consists of several outer reflections and one inner reflection. The spacings corresponding to the outer reflections are essentially those found for the two homopolymers and are independent of the copolymer composition, which we interpret as an indication that the lateral packing in the crystal has a common motif in the homopolymers and copolymers. The spacing corresponding to the inner crystalline reflection various smoothly with copolymer composition, as illustrated for copolymer PB-10,12 in Figure 7, providing further evidence for cocrystallization of the two types of repeating unit. This is more unexpected than the observation of cocrystallization for the PB-5,7 copolymer, since these smectogenic homopolymers appear to have rather well-ordered crystalline phases.

The diffraction pattern of the smectic phase of PB-10,12 was quite clear for all copolymer compositions, indicating that copolymerization does not disrupt the ordered packing in the smectic phase. As shown in Figure 7, the two outer reflections at 4.5 and 5.0 Å are independent of copolymer composition, suggesting that a common mode of lateral packing also exists in the smectic phase. The Bragg spacing of the inner reflection (the smectic layer spacing) is composition dependent and falls above the dashed line representing an arithmetic average of the homopolymer spacings. Thus, it appears that both types of repeating unit can be accommodated in the smectic phase of the copolymers, just as was observed for the mixtures of the corresponding homopolymers.

The enthalpy and entropy changes for the K–S and S–I transitions, as determined from DSC heating curves for three copolymer series, are listed in Table II. Figure 8 shows the entropy changes for PB-10,12 copolymers plotted as a function of copolymer composition. The entropy change for the crystal–smectic transition is significantly depressed by the addition of the second comonomer. If both units cocrystallize, as is the case here, the entropy of the crystalline phase will be raised, and ΔS_{K-S} will be depressed. Hence, the variation of ΔS_{K-S} with copolymer composition cannot be interpreted quantitatively in terms of the degree of crystallinity. By contrast, the variation

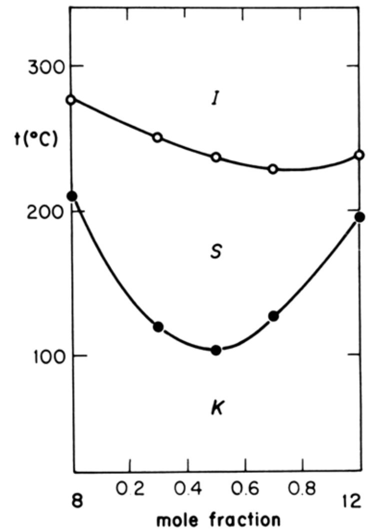

Figure 9. Phase diagram for PB-8,12 copolymers.

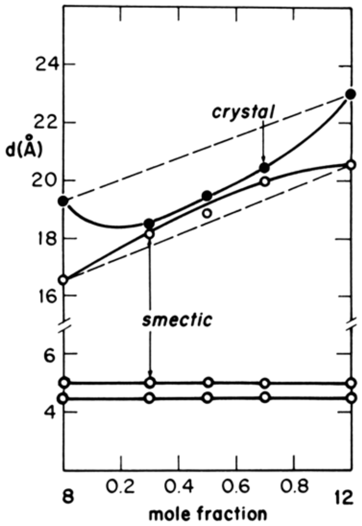

Figure 10. Bragg spacings of the crystalline phase of PB-8,12 copolymers at 25 °C (filled circles) and the smectic phase at 230 °C (open circles).

of the smectic–isotropic transition temperature and the corresponding entropy change very nearly follow the arithmetic averages. We conclude from this observation that incorporation of a second repeating unit of different length does not significantly disrupt the structure of the smectic phase. This is somewhat surprising in this particular case in view of the highly ordered nature of the S_H phase.

3. Copolymer PB-8,12. This even–even copolymer has a larger difference between the two repeating units than the preceding case. Typical DSC curves are illustrated for one composition in Figure 4c. The peaks representing the transitions are broader than those of PB-10,12. The phase diagram in Figure 9 shows a very large depression of the crystal melting temperature upon addition of the second comonomer, so that the temperature span of the smectic phase is broadened to almost 140 °C for the equimolar copolymer. This copolymer exhibits fewer crystalline reflections, as can be seen upon comparison of the entries in Table I for the equimolar copolymers of PB-8,12 and PB-10,12, which signifies poorer crystal perfection. Figure 10 illustrates the composition dependences of the crystal *c*-axis dimensions and the layer spacings of the smectic phase. For this copolymer the negative deviation of the crystal *c* spacing from the arithmetic mean is much more pronounced. In fact, this crystal spacing is only slightly larger than the smectic layer spacing for compositions in the mole fraction range 0.3–0.7.

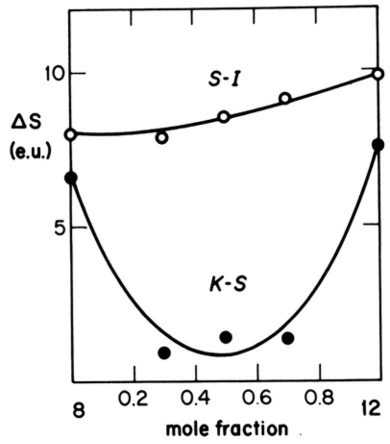

Figure 11. Entropy changes for the crystal–smectic and smectic–isotropic transitions of PB-8,12 copolymers.

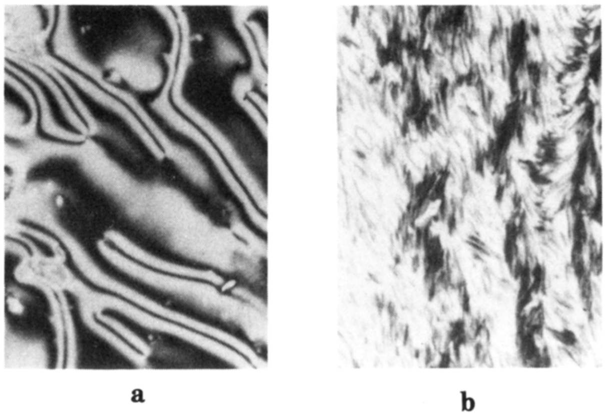

a

b

Figure 12. (a) Schlieren texture observed for the monotropic nematic phase of the copolymer PB-6,12 having 0.3 mol fraction suberate units upon cooling to 220 °C. (b) Fan-shaped texture of the smectic phase found on cooling the same sample at 210 °C.

In contrast to the poorer quality of the crystalline diffraction pattern of these copolymers, the smectic phases of all copolymers gave a well-defined pattern consisting of one inner and two outer reflections. Evidently introduction of a second repeating unit, even one differing substantially in length, is much less disruptive to the smectic phase than to the crystalline phase. Further supporting evidence for this conclusion appears in Figure 11, where the composition dependence of the entropy changes for the K–S and S–I transitions are compared. The decrease of ΔS_{K-S} is even more pronounced for this copolymer than was the case for PB-10,12. We believe that both repeating units enter the crystal lattice in this case also, but the resulting crystal has only short-range order along the chain axis and a much reduced degree of crystallinity.

4. Copolymer PB-6,12. This even–even copolymer has the largest difference in the lengths of the two types of repeating unit. The transitions appearing in the DSC curves shown in Figure 4d are very broad, and the crystal melting temperature could not be determined reliably for a range of compositions near equimolar. It should be noted that the upper temperature transition seen in the heating curve is replaced by two transitions in the cooling curve. This region of the phase diagram could be clarified by use of the polarizing microscope and hot stage. Figure 12a illustrates a typical schlieren texture seen on cooling the 30:70 copolymer to 220 °C, so the additional transition is

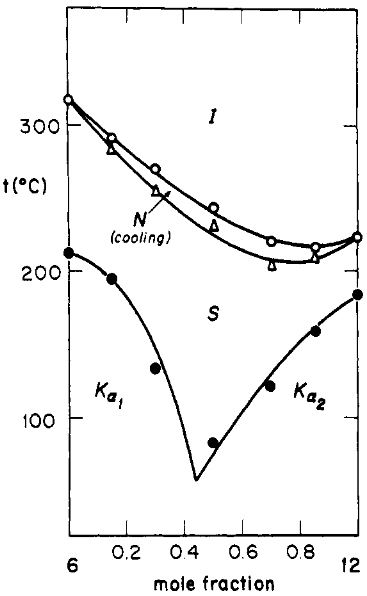

Figure 13. Phase diagram constructed from the DSC cooling curves for PB-6,12 copolymers.

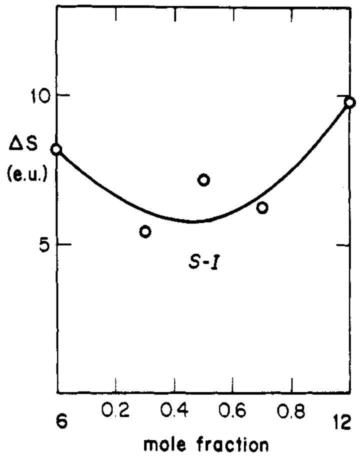

Figure 14. Entropy change for the smectic–isotropic transition of various PB-6,12 copolymers.

due to a monotropic nematic phase. Further cooling to 210 °C produced the fan-shaped smectic texture shown in Figure 12b. When this smectic phase was heated, it was observed to transform directly to the isotropic phase, as expected from the DSC data. Since no evidence of a nematic phase was found for either homopolymer, we conclude that copolymerization with units differing substantially in length destabilizes the smectic phase relative to the nematic mesophase.

The phase diagram for the PB-6,12 copolymers constructed from the cooling curve data appears in Figure 13. In contrast to the preceding copolymers of the even–even type, in this system the crystal–smectic transition exhibits a eutectic. Hence, no cocrystallization occurs when the repeating units are quite different in length. As indicated for the equimolar copolymer in Table I, the diffraction diagram of the crystalline phase shows relatively few reflections, and the inner reflection is missing from the smectic phase. However, the smectic phase is surely present, as indicated by the 4.5- and 5.0-Å reflections common to the smectic phase of these homologues, which are easily distinguished from the 4.28- and 4.73-Å reflections of the crystalline phase. No estimate of the entropy of fusion could be obtained from the broad endotherms seen in the heating curves. Figure 14 illustrates the composition dependence of ΔS_{S-I}. Unlike the previous copolymers, PB-6,12 exhibits a significant depression of ΔS_{S-I} upon addition of the second comonomer. We conclude that the structure of the smectic phase becomes imperfect when it is forced to accept repeating units of widely different lengths. The lack of an inner reflection in the diffraction pattern of this smectic phase further supports this contention.

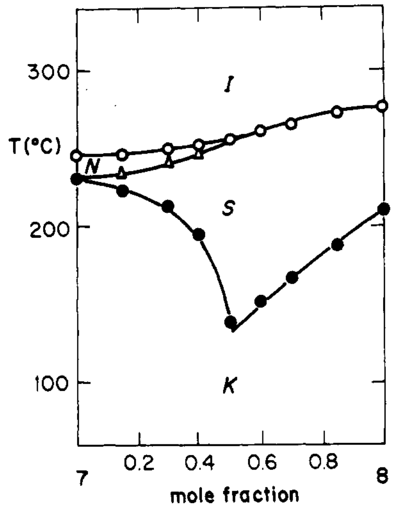

Figure 15. PB-7,8 copolymer phase diagram determined from DSC cooling curves.

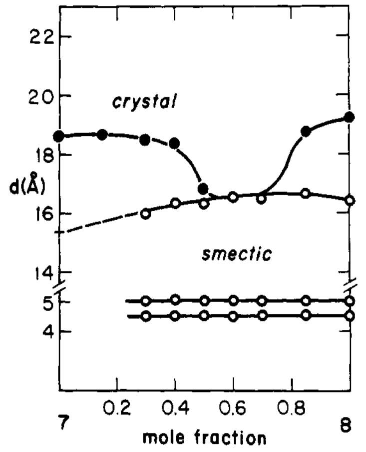

Figure 16. Bragg spacings measured for the crystalline phase at 25 °C (filled circles) and the smectic phase at 230 °C (open circles) for PB-7,8 copolymers.

5. Copolymer PB-7,8. An example of the DSC heating and cooling curves for this copolymer containing both even and odd numbers of methylene units appears in Figure 4e. There are two endotherms in the heating curve and three exotherms in the cooling curve. A schlieren texture confirmed that the monotropic phase is nematic. Figure 15 shows the phase diagram constructed from the DSC cooling curves. Although the nematic phase appears to extend almost across the full composition range in this phase diagram, the nematic phase is monotropic for copolymers having less than 60 mol % azelate units.

The crystal melting temperatures exhibit a eutectic, indicating the presence of distinct crystal structures for the two types of units. There is a suggestion that a third type of crystal may occur for sebacate compositions somewhat greater than equimolar. The Bragg spacings measured for the crystalline and smectic phases are illustrated in Figure 16. Those for the smectic phase show the same features seen in the other copolymers. The 4.5- and 5.0-Å spacings are independent of copolymer composition, while the layer spacing falls above the line representing the arithmetic average of the spacing calculated

Table III
Enthalpies and Entropies of Transition for Azelate and Sebacate Copolymers[a]

polymer	$\Delta H_{K\text{-}S}$	$\Delta H_{S\text{-}N}$	$\Delta H_{N\text{-}I}$	$\Delta H_{K\text{-}I}$	$\Delta S_{K\text{-}S}$	$\Delta S_{S\text{-}N}$	$\Delta S_{N\text{-}I}$	$\Delta S_{K\text{-}I}$
PB7	1.6	1.1^5	0.8	3.5^5	3.1^5	2.2^5	1.5^5	6.9^5
85:15	0.5	2.0	0.9	3.4	1.1	3.9	1.7	6.7
70:30	0.8	1.7[b]	1.1[b]	3.6	1.7	3.4[b]	2.2[b]	7.3
60:40	0.9	1.6[b]	1.3[b]	3.8	1.8	3.1[b]	2.4[b]	7.3
50:50	1.0	2.0[b]	1.1[b]	4.1	2.5	3.9[b]	2.1[b]	8.5
40:60	0.8	1.6[b]	1.3[b]	3.7	1.8	3.1[b]	2.4[b]	7.3
30:70	1.0	3.5		4.5	2.3	6.4		8.7
15:85	1.9	3.8		5.7	4.2	7.0		11.2
PB8	3.3	4.5		7.8	6.6	8.0		14.6

[a] ΔH values are in kcal/mol. ΔS values are in cal mol^{-1} K^{-1}. [b] Determined from areas of exotherms in DSC cooling curves.

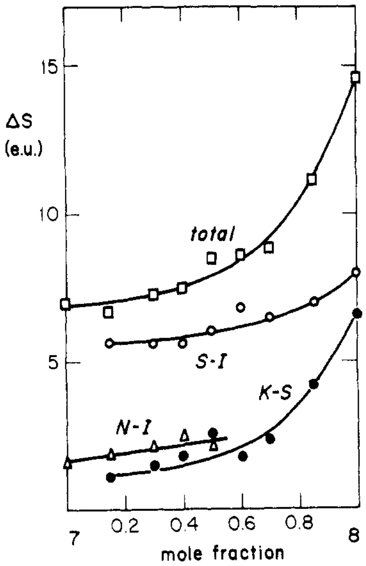

Figure 17. Total entropy change for the crystal–isotropic transition and for the smectic–isotropic, nematic–isotropic, and crystal–smectic transitions for PB-7,8 copolymers.

for the hypothetical smectic phase of PB7 and the one observed for PB8. Evidence for a smectic phase was obtained for copolymers having a sebacate composition as low as 10 mol %, but the narrow temperature interval of the smectic phase for these compositions precluded X-ray study. The c-axis spacing varies discontinuously with copolymer composition and is nearly the same as the smectic layer spacing for 50–70 mol % sebacate units. We conclude that the two types of units crystallize separately at the two extremes of copolymer composition, while a new crystal form appears in those copolymers which are nearly equimolar.

The entropy changes for the PB-7,8 copolymers are listed in Table III and appear plotted against the mole fraction of sebacate units in Figure 17. The overall entropy change from the crystalline solid to the isotropic liquid, ΔS_{total}, decreases markedly upon addition of azelate units. This is primarily due to a reduction of the degree of crystallinity, as reflected by the decrease in $\Delta S_{K\text{-}S}$. The increase in $\Delta S_{N\text{-}I}$ with increasing mole fraction of sebacate may reflect an increase in the order of the nematic phase, while the more pronounced decrease of $\Delta S_{S\text{-}I}$ with increasing azelate composition indicates that the smectic phase becomes more disordered as azelate units are incorporated.

Discussion

According to Flory,[16] the depression of the melting temperature of crystallizable A units by random copolymerization with noncrystallizable B units is given by

$$\frac{1}{T_M} - \frac{1}{T_M{}^0} = -\frac{R}{\Delta H_f} \ln x_A \qquad (1)$$

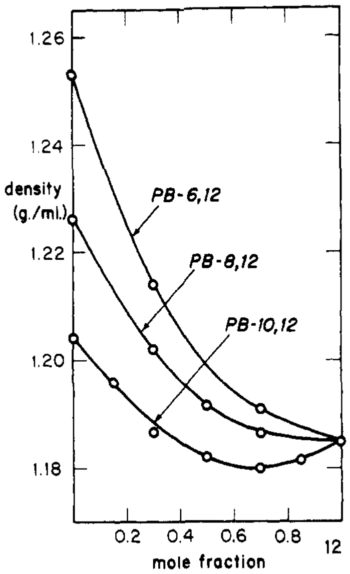

Figure 18. Densities measured at room temperature for the crystalline phases of copolymers PB-6,12, PB-8,12, and PB-10,12.

where ΔH_f is the heat of fusion per mole of A repeating units and x_A is their mole fraction in the copolymer. If both units crystallize separately and independently, a eutectic behavior is predicted. Fairly exhaustive data for non-mesogenic random copolyamides and copolyesters have been reviewed by Mandelkern.[17] The composition dependence of the melting depression is satisfactorily accounted for by the above relation, but the values of ΔH_f deduced from copolymer melting depressions are frequently significantly smaller than those derived from melting depressions caused by small-molecule diluents. Incorporation of copolymer units broadens the melting transition and decreases the degree of crystallinity. The recorded melting temperature depends strongly upon how sensitive the detection method is to the present of the last residual crystallinity, since this disappears over a significant temperature range. Mandelkern attributes the discrepancy between ΔH_f values to this cause. He also cites several examples in which two copolymer units cocrystallize, in which case the composition dependence of the melting temperature is smooth and no eutectic exists. For some of the examples cocrystallization is not surprising since the two units have geometric similarities, but in the case of styrene and poly(p-fluorostyrene) the two units cocrystallize even though the homopolymers exhibit different crystal symmetry.[18]

Figure 4 provides evidence that copolymerization also broadens the crystal melting transitions of mesogenic copolymers. As shown in Figure 18, the densities of the copolymers fall significantly below the arithmetic averages for the two homopolymers. We interpret this result, in conjunction with the observed decrease in the entropies of fusion, as indicating a lower degree of crystallinity in the copolymers. The amount of broadening of the melting transition, and lowering of the crystal melting temperature, increases as the difference between the repeating units increases. In the present system differences in both the length of the repeating unit and even–odd character are important. Both small-molecule and homopolymeric mesogens are notable for the frequent occurrence of crystalline polymorphism. This indicates that two or more crystal forms having comparable free energy is a common occurrence for this class of materials. One might anticipate from this observation that cocrystallization might occur frequently in binary mixtures of mesogens. Among the systems studied here, cocrystallization is indicated by the phase diagrams of the copolymers PB-5,7, PB-10,12, and PB-8,12. A eutectic is found for mixtures of PB 5 and PB7, for the PB-6,12 copolymer (in which the two units differ substantially in length), and for the PB-7,8 copolymer (involving both odd and even numbers of methylene units in the dibasic acids). However, in the latter example, as well as the mixture of PB10 and PB12, there is ome evidence for a third crystal modification over a limited composition range near equimolar. This latter crystal form, in all probability, incorporates both types of repeating unit. Clearly, the frequency of cocrystallization is the major difference between the crystalline phases of mesogens and non-mesogens.

Our results indicate that both nematic and smectic mesophases can accommodate different units of the same mesogenic type with minimal disruption of the mesophase structure. This observation is not unexpected for the nematic phase which exhibits only one-dimensional orientational order, but it is somewhat surprising for the more highly ordered smectic S_H phase. Only the PB-6,12 copolymers, in which the units are quite different in length, show a significant reduction of $\Delta S_{S\text{-}I}$ for compositions near equimolar. It is not evident how units of different length are accommodated within the regular layer structure; however, the diffraction results demand a well-ordered layer structure for the smectic phases of all copolymers except PB-6,12. The layer spacing of the smectic phase of copolymers is always larger than the arithmetic average, which may mitigate the disrupting effect of the units of different lengths. Another possibility is that rotational isomerism of the methylene units in the flexible segment may act to make the two units more similar in length. Such random variation may be tolerated in the liquid crystal structure, whereas it could not occur in the crystal phase. This might explain why copolymerization disrupts the structure of the crystalline phase much more than that of the liquid crystal. Lydon and Coakley[19] investigated mixtures of the low molecular weight compounds 4′-*n*-octyl-4-cyanobiphenyl and 2-((4-((*n*-octadecyl)oxy]benzylidene)amino]fluorene, both of which form a smectic S_A phase. They found the layer spacing for the mixtures varies smoothly between 30 and 36 Å and concluded from this variation, plus the lack of broadening of the inner reflection for the mixtures, that the components are randomly mixed within each layer.

In conclusion, we have observed that copolymerization lowers the crystal–mesophase transition temperature and increases the temperature range of the mesophase. These effects become more pronounced if the copolymer units differ significantly in length or in even–odd character. Moreover, the PB-6,12 copolymer exhibited a monotropic nematic phase not present in either homopolymer, providing an unexpected example of polymesomorphism. The results reported in this paper apply only to copolymers involving two different flexible segments, and one might anticipate different results for copolymers in which the rigid unit is varied.

Acknowledgment. We express our appreciation to the National Science Foundation Division of Materials Research and the Industry–University Cooperative Research Program for support of this work on Grant DMR-81-06160.

References and Notes

(1) de Gennes, P.-G. *C. R. Hebd. Seances Acad. Sci., Ser. B* **1975**, *281*, 101.

(2) Roviello, A.; Sirigu, A. *J. Polym. Sci., Polym. Lett. Ed.* **1975**, *13*, 455.

(3) van Luyen, D.; Liébert, L.; Strzelecki, L. *Eur. Polym. J.* **1980**, *16*, 307.

(4) Asrar, J.; Toriumi, H.; Watanabe, J.; Krigbaum, W. R.; Ciferri, A. *J. Polym. Sci., Polym. Phys. Ed.* **1983**, *21*, 1119.

(5) Krigbaum, W. R.; Watanabe, J.; Ishikawa, T. *Macromolecules* **1983**, *16*, 1271.

(6) Bosio, L.; Fayolle, B.; Frederich, C.; Laupretre, F.; Meurisse, P.; Noel, C.; Virlet, J. In "Liquid Crystals and Ordered Fluids"; Griffin, A., Johnson, J., Eds; Plenum Press: New York, 1983; Vol. 4.

(7) Galli, G.; Chielli, E.; Ober, C. K.; Lenz, R. W. *Makromol. Chem.* **1982**, *183*, 2693.

(8) Arnold, H.; Sackmann, H. *Z. Phys. Chem. (Leipzig)* **1960**, *213*, 145.

(9) Sackman, H.; Demus, D. *Mol. Cryst. Liq. Cryst* **1973**, *21*, 239.

(10) Sackman, H. In "Liquid Crystals of One- and Two-Dimensional Order"; Helfrich, W., Heppke, G., Eds.; Springer-Verlag: Berlin, 1980, p 19.

(11) Krigbaum, W. R.; Ciferri, A.; Asrar, J.; Toriumi, H.; Preston, J. *Mol Cryst. Liq. Cryst.* **1981**, *76*, 79.

(12) Krigbaum, W. R.; Asrar, J.; Toriumi, H.; Ciferri, A.; Preston, J. *J. Polym. Sci., Polym. Lett. Ed.* **1982**, *10*, 109.

(13) Krigbaum, W. R.; Ishikawa, T.; Watanabe, J.; Toriumi, H.; Kubota, K.; Preston, J. *J. Polym. Sci., Polym. Phys. Ed.* **1983**, *21*, 1851.

(14) Krigbaum, W. R.; Watanabe, J. *Polymer* **1983**, *24*, 1299.

(15) Krigbaum, W. R.; Kotek, R.; Ishikawa, T.; Hakemi, H.; Preston, J. *Eur. Polym. J.* **1984**, *20*, 225.

(16) Flory, P. J. *J. Chem. Phys.* **1947**, *15*, 684; **1949**, *17*, 223.

(17) Mandelkern, L. "Crystallization of Polymers"; McGraw-Hill: New York, 1964; Chapter 4.

(18) Natta, G. *Macromol. Chem.* **1960**, *35*, 94.

(19) Lydon, J. E.; Coakley, C. J. *J. Phys. (Orsay, Fr.)* **1975**, *36 (C-1)*, 45.